Published in final edited form as:
*J Bone Miner Res*. 2012 February ; 27(2): 374–389. doi:10.1002/jbmr.548.

# Cell autonomous requirement of connexin 43 for osteocyte survival: consequences for endocortical resorption and periosteal bone formation

**Nicoletta Bivi**[1], **Keith W. Condon**[1], **Matthew R. Allen**[1], **Nathan Farlow**[1], **Giovanni Passeri**[1,§], **Lucas R. Brun**[1,@], **Yumie Rhee**[1,#], **Teresita Bellido**[1,2], and **Lilian I. Plotkin**[1,*]

[1]Dept. Anatomy & Cell Biology, Indiana University School of Medicine, U.S.A.

[2]Dept. Internal Medicine, Div. Endocrinology, Indiana University School of Medicine, U.S.A.

## Abstract

Connexin 43 (Cx43) mediates osteocyte communication with other cells and with the extracellular milieu and regulates osteoblastic cell signaling and gene expression. We now report that mice lacking Cx43 in osteoblasts/osteocytes or only in osteocytes ($Cx43^{\Delta Ot}$ mice) exhibit increased osteocyte apoptosis, endocortical resorption and periosteal bone formation, resulting in higher marrow cavity and total tissue areas measured at the femoral mid-diaphysis. Blockade of resorption reversed the increased marrow cavity but not total tissue area, demonstrating that endocortical resorption and periosteal apposition are independently regulated. Anatomical mapping of apoptotic osteocytes, osteocytic protein expression, and resorption and formation, suggests that Cx43 controls osteoclast and osteoblast activity by regulating osteoprotegerin and sclerostin levels, respectively, in osteocytes located in specific areas of the cortex. Whereas empty lacunae and living osteocytes lacking osteoprotegerin were distributed throughout cortical bone in $Cx43^{\Delta Ot}$ mice, apoptotic osteocytes were preferentially located in areas containing osteoclasts, suggesting that osteoclast recruitment requires active signaling from dying osteocytes. Furthermore, Cx43 deletion in cultured osteocytic cells resulted in increased apoptosis and decreased osteoprotegerin expression. Thus, Cx43 is essential in a cell-autonomous fashion *in vivo* and *in vitro* for osteocyte survival and for controlling the expression of osteocytic genes that affect osteoclast and osteoblast function.

### Keywords

connexin 43; apoptosis; osteocyte; osteoblast; bone resorption; osteoprotegerin; SOST/sclerostin; periosteal bone formation

## INTRODUCTION

Mounting evidence from recent years demonstrates that the concerted actions of bone forming osteoblasts and bone resorbing osteoclasts, which are responsible for maintaining the mass and geometry of the skeleton, are modulated by signals originating from

[*]**Corresponding author:** Lilian I. Plotkin, Ph.D. Department of Anatomy and Cell Biology Indiana University School of Medicine 635 Barnhill Drive, MS-5035 Indianapolis, IN 46202-5120 Phone: 1-317-274-5317 Fax: 1-317-278-2040 lplotkin@iupui.edu.
[§]Current address: Dept Internal Medicine and Biomedical Sciences, Center for Metabolic Bone Diseases, University of Parma, Parma, Italy
[@]Current address: Laboratory of Bone Biology and Mineral Metabolism, School of Medicine, University of Rosario, Santa Fe, Argentina
[#]Current address: Dept. Internal Medicine, Yonsei University College of Medicine, Seoul, Korea

osteocytes. Osteocytes are terminally differentiated osteoblasts that become entombed during the process of bone deposition and reside embedded in the mineralized matrix, but remain highly communicated among themselves and with other cellular elements on the bone surface, the bone marrow, and the vasculature [1]. Sclerostin, the product of the *SOST* gene expressed in osteocytes, is one of the recognized molecular mediators by which osteocytes modulate the function of the cells that remodel bone [2]. Because sclerostin is a potent inhibitor of bone formation, changes in its expression in human diseases or in response to hormonal and mechanical stimuli, have a profound impact on bone mass. Osteocytes also express proteins that modulate osteoclast formation and activity such as the receptor activator of NF-κB (RANKL) and its decoy receptor osteoprotegerin (OPG) [3,4]. Moreover, overexpression of a constitutively active parathyroid hormone receptor 1 or deletion of the Wnt canonical signaling mediator β-catenin in osteocytes, results in increased RANKL/OPG ratio, osteoclast activity, and bone resorption [4-6]. In addition, loss of osteocyte viability induced by either too high or too low mechanical strains, by decreased levels of sex hormones, or by genetically-induced osteocyte death, temporally precedes and is spatially associated with osteoclast recruitment to the same location, a concept known as targeted remodeling [7-11]. However, it remains unknown whether osteoclastogenic cytokines, other products derived from osteocytes, or apoptotic osteocytic bodies are responsible for this phenomenon.

Channels formed by connexin 43 (Cx43), the most abundant member of the connexin family of proteins expressed in bone cells, mediate the communication among osteocytes and between osteocytes and cells on the bone surface [12]. Gap junction channels established between neighboring cells and hemichannels expressed in unopposed cell membranes allow the passage of small size (<1 kDa) molecules among cells or between cells and their extracellular milieu [13]. Besides its participation in gap junctions and hemichannels, Cx43 might also affect osteoblast and osteocyte functions by interacting with structural and signaling molecules, thereby modulating intracellular signaling and gene expression [14]. One of the best studied Cx43-interacting proteins is the kinase Src, an upstream regulator of ERKs, which is required for the Cx43-dependent anti-apoptotic effect of bisphosphonates on osteoblasts and osteocytes [15,16]. Cx43 also interacts with β-arrestin, a modulator of G protein-coupled receptors, and this association is indispensible for cAMP-mediated responses downstream of the parathyroid receptor 1 in osteoblasts [17]. Moreover, Cx43 modulates gene transcription in osteoblasts *in vitro* by altering transcription factor recruitment to connexin response elements present in osteoblast-specific genes, such as osteocalcin [18].

Several animal models have been developed to investigate the function of Cx43 in bone forming cells *in vivo* and have demonstrated that lack of Cx43 expression is necessary at an early stage during osteoblast differentiation. Thus, mice lacking Cx43 in osteochondroprogenitors developed using the Dermo1 promoter to drive Cre recombinase [19] or in early osteoblasts using the Col1-2.3kb promoter [20] have delayed mineralization and low bone mass, due to decreased osteoblast differentiation and function. A similar bone phenotype has been reported when Cx43 function is disrupted by overexpressing the mutant oculodentodigital dysplasia (ODDD) Gja1 allele under the control of the Dermo1 promoter [19]. These mouse models of Cx43 deletion exhibit changes in the geometry of long bones resulting in tubular-like shape, which is also present in patients with ODDD [21]. This can be hardly explained by defective osteoblast differentiation, raising the possibility that part of the phenotype of mice in which Cx43 was deleted using the early promoters (Dermo1 and Col1-2.3kb) is due to the contribution of more mature osteoblasts and in particular of osteocytes.

In the current study we investigated the consequences of Cx43 deletion in osteocytes *in vivo* using mice in which Cx43 was deleted from both mature osteoblasts and osteocytes using the human osteocalcin (OCN) promoter [22] or exclusively from osteocytes using the dentin matrix protein 1 (DMP1)-8kb promoter. We found that lack of Cx43 expression exclusively in osteocytes is sufficient to elicit the long bone phenotype observed in the aforementioned animal models. Moreover, we showed that bone formation and resorption are associated with a marked increase in osteocyte apoptosis. These changes in the activity of osteoclasts and osteoblasts result from an osteocyte cell autonomous decrease in OPG expression and a reduction in sclerostin-expressing osteocytes as a consequence of the loss of viable cells. In conclusion, our findings provide support for the intrinsic role of Cx43 in the control of bone formation and resorption specifically by osteocytes and in the maintenance of osteocyte viability.

## MATERIALS AND METHODS

### Mice

Mice with deletion of Cx43 from osteocytes and osteoblasts ($Cx43^{\Delta Ob\text{-}Ot/-}$) or exclusively from osteocytes ($Cx43^{\Delta Ot}$) were generated using the Cre/LoxP system [23,24]. $Cx43^{\Delta Ob\text{-}Ot/-}$ mice and $Cx43^{fl/-}$ control littermates were generated by crossing mice homozygous for the floxed Cx43 gene ($Cx43^{fl/fl}$ mice) [25], generated by K. Willecke, Universitat Bonn, Bonn, Germany, or $Cx43^{+/-}$ mice [26], generated by J. Rossant, University of Toronto, ON, Canada, to facilitate the complete deletion of Cx43 in osteocytes and osteoblasts. $Cx43^{fl/-}$ mice were then crossed with mice expressing Cre recombinase driven by the human osteocalcin promoter (OCN-Cre mice) [27], generated by T. Clemens, Johns Hopkins University School of Medicine, Baltimore, MA. Effective deletion of Cx43 from osteoblasts and osteocytes in these mice was demonstrated earlier by a reduction in Cx43 mRNA of 70%, as determined by qPCR in cultured calvaria cells, and the lack of Cx43 protein expression demonstrated by immunostaining in bone sections [22]. Female mice at 4.5 months of age (n=6-11 per group) were administered daily subcutaneous injections of 0.75 mg/kg alendronate or the equivalent volume of saline for 31 days, as previously published [22].

To delete Cx43 from osteocytes only, we generated $Cx43^{\Delta Ot}$ mice. In this case, we used $Cx43^{fl/fl}$ mice, instead of $Cx43^{fl/-}$, since more recent evidence demonstrated efficient deletion of Cx43 also using $Cx43^{fl/fl}$ mice [28]. $Cx43^{\Delta Ot}$ mice and $Cx43^{fl/fl}$ control littermates were generated by crossing $Cx43^{fl/fl}$ mice with DMP1-8kb-Cre mice, which express Cre recombinase under the control of a 12kb DNA fragment containing 8 kb of the 5′-flanking region, the first exon, the first intron, and 17bp of exon 2 of the murine DMP1 gene [29]. DMP1-8kb-Cre mice were produced by microinjection of purified DNA into pronuclei of C57BL/6 mice at the transgenic mouse core facility of the University of Arkansas for Medical Sciences. $Cx43^{\Delta Ot}$ mice and $Cx43^{fl/fl}$ control littermates are genetically similar, since both $Cx43^{fl/fl}$ and DMP1-8kb-Cre mice were generated in a C57BL/6 background.

Mice were genotyped by PCR using specific primer sets [25,27,30,31]. The presence of the deleted allele of Cx43 and endogenous DMP1 was evaluated by PCR in genomic DNA extracted from brain, kidney, heart, skeletal muscle (gastrocnemius), and bone (tibia), as described elsewhere [5,20]. Mice were born at the expected Mendelian frequency, were fertile, and exhibited normal size and weight. Female mice at 4.5 months of age (n=6-11 per group) were used for the phenotypic analysis. For the longitudinal BMD studies, female mice between 1 and 4 month of age (n=9-17 per group) were used. Protocols involving mice were approved by the Institutional Animal Care and Use Committee of Indiana University School of Medicine

### Bone dynamic histomorphometry

Mice were injected intraperitoneally with tetracycline HCl or calcein (30 mg/kg, Sigma Chemical, St. Louis, MO) 7 and 3 days before sacrifice, as previously described [7]. Fluorochrome labels were quantified using Bioquant OSTEO 7.20.10 (Bioquant Image Analysis Co., Nashville, TN) or OsteoMeasure High Resolution Digital Video System (OsteoMetrics, Inc., Decatur, GA) [32,33]. A value of 0.1 μm/day was used for mineral apposition rate (MAR) when only single label was present in order to allow calculation of bone formation rate (BFR/BS) [34]. Analyses were performed on longitudinal femoral 5 μm-thick sections from the midshaft up to 2.5 mm towards the distal end or on 150 μm-thick cross-sections at the middiaphysis, in order to evaluate the anatomical distribution of the histological parameters. The terminology and units are those recommended by the Histomorphometry Nomenclature Committee of the ASBMR [35].

### Transmission electron microscopy (TEM)

Femoral midshaft cross-sections were decalcified and post-fixed in 2% paraformaldehyde/ 2% glutaraldehyde in 0.1M cacodylate buffer for 1h, followed by 1h-treatment with 1% osmium tetroxide in 0.1M cacodylate buffer. The bone specimens were then dehydrated, embedded in Embed 812 resin (Electron Microscopy Sciences, Hatfield, PA), and thin sectioned using a Diatome diamond knife (Electron Microscopy Sciences, Hatfield, PA) at a thickness of 70-90 nm. Sections were placed on copper grids, stained with uranyl acetate, and viewed on a Tecnai G2 12 Bio Twin electron microscope (FEI, Hillsboro, OR) at the Electron Microscopy Center of the Department of Anatomy and Cell Biology (Indiana University School of Medicine). Digital images were taken with an Advanced Microscope Techniques (Danvers, MA) CCD camera.

### Bone turnover markers

Plasma osteocalcin (OCN) was measured using enzyme radiometric or linked immunoadsorbent assays (Biomedical Technologies, Soughton, MA), as published [6,33]. Plasma C-telopeptide fragments of type I collagen (CTX) were measured using an enzyme linked immunoadsorbent assay (RatLaps, Immunodiagnostic Systems Inc., Fountain Hills, AZ), as published [33].

### Bone mineral density (BMD) and micro-computed tomography (μCT) analysis

BMD of the total body (excluding the head), of the spine (L1-L6), and femur was determined by dual energy x-ray absorptiometry (DXA) using a PIXImus II densitometer (G.E. Medical Systems, Lunar Division, Madison, WI), as previously described [5]. For μCT analysis, femora were dissected, cleaned of soft tissue, fixed, and stored in 70% ethanol until analyzed at 6 μm resolution using a Skyscan 1172 instrument (SkyScan, Kontich, Belgium) [5].

### Calvaria cell isolation

Osteoblastic cells were obtained from calvarial bones of neonatal mice and cultured at an initial density of $5\times10^4/cm^2$ for 6 days in the presence of α-MEM supplemented with 10% fetal bovine serum and 50μg/ml ascorbic acid, as published.[22,36] Half of the medium was replaced by fresh medium every other day.

### Osteocyte isolation and osteocyte-enriched bone preparation

Calvaria cells were isolated from double transgenic mice DMP1-8kb-GFP/DMP1-8kb-Cre. GFP-expressing cells (osteocyte-enriched) were separated from GFP-negative cells (osteoblast-enriched) by sorting the cell suspension using a FACSAria flow cytometer (BD Biosciences, Sparks, MD) at the Indiana University Flow Cytometry Core Facility [5]. To

obtain mRNA from osteocyte-enriched bone preparations, the epiphyses of the femora and tibiae were cut off, the bone marrow was flushed out using phosphate buffered saline, and the periosteum was mechanically removed. The obtained diaphyses were then digested 4 times (one hour each) to further remove osteoblastic cells with a mixture of 1.5U/ml Collagenase P (Roche Applied Science, Indianapolis, IN), 0.05% Trypsin and 1mM EDTA (Invitrogen, Carlsbad, CA), as published by Kramer et al [4], with modifications.

**RNA extraction and quantitative PCR (*qPCR)*—**RNA was purified using Ultraspec (Biotecx Laboratories, Houston, TX) or SurePrep RNA isolation kit (Fisher scientific, Pittsburgh, PA). qPCR was performed as described [5], using the house-keeping genes mitochondrial ribosomal protein S2 (Mrps2) or glyceraldehyde 3-phosphate dehydrogenase (GAPDH), and the ΔCt method [5]. Primers and probes for floxed-Cx43, CRE recombinase and RANKL were manufactured by Assays-by-Design (Applied Biosystems, Foster City, CA). The remaining primers were designed using the Assay Design Center (Roche Applied Science, Indianapolis, IN) or were commercially available (Applied Biosystems, Foster City, CA).

**Western Blot analysis—**Protein lysates from MLO-Y4 cells were prepared as previously reported [15,37]. Proteins were separated on 10% SDS-polyacrylamide gels and electrotransferred to polyvinylidene difluoride membranes. Immunoblottings were performed using rabbit anti-Cx43 (Sigma, St. Louis, MO) or rabbit anti-ERK1/2 (Santa Cruz Biotechnology, Santa Cruz. CA), followed by anti-rabbit antibodies conjugated with horseradish peroxidase (Santa Cruz Biotechnology, Santa Cruz, CA). The intensity of the bands was quantified using the Fotodyne system (Hartland, WI).

## TUNEL, immunohistochemistry and TRAP staining

Longitudinal sections of the femora were used to analyze $Cx43^{\Delta Ob\text{-}Ot}$ mice, and transversal sections were used for $Cx43^{\Delta Ot}$ mice with the purpose of spatially map the changes in osteocytes, osteoblasts and osteoclasts within the cortical bone. Osteocyte apoptosis was detected by TdT-mediated dUTP nick-end labeling (TUNEL) using a modified version of a commercial kit (Calbiochem, Gibbstown, NJ) in sections counterstained with 2% methyl green, as previously described [22]. Longitudinal sections were used to determine the expression of Cx43 using anti-Cx43 antibodies (Sigma Chemical Co., St. Louis, MO) in the distal femora [22]. Consecutive 5 μm-thick sections at the mid-diaphysis were used for immunohistochemistry with anti-sclerostin antibodies (R&D Systems, Minneapolis, MN) [6], or anti-RANKL and anti-OPG antibodies (Santa Cruz Biotechnology Inc, Santa Cruz, CA) with prior antigen retrieval (DeCal Retrieval Solution, BioGenex, San Ramon, CA) and followed by signal amplification (ABC kit, Vector laboratories, Burlingame, CA). Non-immune IgG was used as negative control. To visualize osteoclasts on the endocortical surface, sections were stained for TRAP, as previously described [38]. Only TRAP-positive cells containing >1 nucleus were counted. Bone sections were scored in two anatomical regions: the outer half (defined as periosteal, Ps) and inner half (defined as endocortical, Ec). Osteocyte parameters were separately assessed in four regions, two comprising the entire anterior and posterior regions defined by a 140°-angle from the center of the bone, and two containing the lateral and medial regions. All the results were reproduced in a separate cohort of 5 $Cx43^{fl/fl}$ and 5 $Cx43^{\Delta Ot}$ animals.

## Cell viability, apoptosis, and proliferation assays and gene expression in cultured cells

MLO-Y4 cells in which Cx43 expression was silenced using MISSION short hairpin RNA Lentiviral Particles (Sigma Chemical Co, Saint Louis, MO) were cultured as published [22]. Wild type UMR-106 osteoblastic cells and UMR-106 cells stably transfected with Cx43 were cultured as published [16]. MTT assay and Trypan blue uptake were performed as

previously described [15,39]. BrdU incorporation was performed using the BrdU Cell proliferation ELISA kit (Exalpha Biologicals, Inc., Shirley, MA) following the manufacturer's instructions. Gene expression was measured by qPCR as indicated above.

### Statistical analysis

All values are reported as the mean ± standard deviation (SD) and were analyzed using SigmaStat (SPSS Science, Chicago, IL). Data were analyzed by two-way ANOVA or *t*-test to address specific questions. Specifically, for **Fig. 1**, two-way ANOVA was performed to establish the synergy between genotype and alendronate treatment. If a significant main effect or interaction was found, we examined it closely by performing Pairwise Multiple Comparisons with Bonferroni correction [40].

## RESULTS

### Mice lacking Cx43 from osteoblasts and osteocytes ($Cx43^{\Delta Ob\text{-}Ot/-}$ mice) exhibit increased osteocyte apoptosis in cortical bone and elevated endocortical resorption and periosteal bone formation

Prompted by evidence that mice lacking Cx43 in osteoblasts and osteocytes ($Cx43^{\Delta Ob\text{-}Ot/-}$) exhibited increased osteocyte apoptosis in the cortical shell of the lumbar vertebrae, but not in the cancellous compartment [22], we investigated whether the prevalence of osteocyte apoptosis was also high in the diaphysis of the femur, a site entirely composed of cortical bone. Female $Cx43^{\Delta Ob\text{-}Ot/-}$ mice at 5.5 months of age exhibited a 2.5-fold increase in the percentage of apoptotic osteocytes, assessed by TUNEL, and a 6-fold increase in the percentage of empty lacunae, another sign of osteocyte death [41], compared to $Cx43^{fl/-}$ control littermates (**Fig. 1A**). Qualitative evaluation by TEM showed features of apoptosis, including chromatin condensation and nuclear fragmentation, in osteocytes from $Cx43^{\Delta Ob\text{-}Ot/-}$ mice, whereas osteocyte nuclei in control mice exhibited normal appearance (**Fig. 1B**). Increased osteocyte apoptosis in $Cx43^{\Delta Ob\text{-}Ot/-}$ mice was associated with a 2.5-fold higher number of osteoclasts (NOc/BS) and bone surface covered by osteoclasts (OcS/BS) on the endocortical surface (**Fig. 1C)**. Bone formation rate (BFR/BS), mineral apposition rate (MAR), and mineralizing surface (MS/BS) on the periosteal surface were all higher in $Cx43^{\Delta Ob\text{-}Ot/-}$ mice compared to $Cx43^{fl/-}$ control littermates (**Fig. 1D**), whereas on the endocortical surface these indexes of bone formation were not different between groups (**Fig. 1E**). Circulating osteocalcin levels were, however, lower in vehicle-treated $Cx43^{\Delta Ob\text{-}Ot/-}$ mice compared to control littermates (**Fig. 1F**). This is likely the systemic expression of a generalized reduction in osteoblast activity due to removal of Cx43 from osteblasts, as previously shown [20,42].

As a result of the enhanced osteoclast presence on the endocortical surface and increased bone formation on the periosteal surface, $Cx43^{\Delta Ob\text{-}Ot/-}$ mice exhibited geometric changes characterized by larger marrow cavity and total tissue area, without changes in cortical thickness, measured by μCT (**Table 1**). However, unlike mice in which Cx43 was deleted using the 2.3kb fragment of the col1a1 promoter [20], $Cx43^{\Delta Ob\text{-}Ot}$ mice did not display low bone mass or impaired mineralization ([22] and **Table 1**), indicating that bone mass is preserved when Cx43 is deleted at a later stage during osteoblast differentiation. The distribution of cortical bone in a wider cross-section resulted in an increased minimum moment of inertia (Imin). Consistent with our previous findings in vertebral bone [22], cancellous bone microarchitecture in the distal femur was not affected by Cx43 deletion (**Table 2**).

We next examined whether the elevated periosteal apposition in $Cx43^{\Delta Ob\text{-}Ot/-}$ mice was a compensatory consequence of the increased endocortical resorption or whether they were

independent effects of Cx43 deletion. To this end, we evaluated the effect of inhibiting bone resorption with alendronate on the increased periosteal bone formation observed in $Cx43^{\Delta Ob\text{-}Ot/-}$ mice. Osteoclasts were not reduced and indeed were increased in bisphosphonate-treated animals (**Fig. 1C**), likely due to accumulation of inactive osteoclasts, as found in humans treated with bisphosphonates [43]. However, osteocalcin was markedly decreased in the circulation of both control and Cx43 deficient mice, indicating an effective inhibition of bone turnover by the bisphosphonate (**Fig. 1F**). MS/BS and bone formation rate on the endocortical surface of control and conditional knock-out mice were also reduced in alendronate-treated animals (**Fig. 1E**). This resulted in a reduction in the marrow cavity area in $Cx43^{\Delta Ob\text{-}Ot/-}$ mice treated with alendronate to reach values comparable to those found in control mice (**Table 1**). Alendronate also decreased periosteal BFR/BS in both Cx43 deficient and control mice (**Fig. 1D**). However, the periosteal surface covered by osteoblasts and periosteal bone formation rate remained higher in $Cx43^{\Delta Ob\text{-}Ot/-}$ mice treated with alendronate. Due to the inhibition of endocortical resorption without blocking periosteal apposition, cortical area and thickness were increased by alendronate administration to both control and $Cx43^{\Delta Ob\text{-}Ot/-}$ mice (**Table 1**). These findings are consistent with the regulation of endocortical resorption and periosteal apposition by Cx43 through independent mechanisms.

## Removal of Cx43 exclusively from osteocytes in $Cx43^{\Delta Ot}$ mice is sufficient to induce changes in femoral geometry and increase osteocyte apoptosis

To investigate whether the increased bone formation and resorption and osteocyte apoptosis in $Cx43^{\Delta Ob\text{-}Ot}$ mice are caused by the removal of Cx43 from osteocytes or whether they are secondary to the lack of the protein in osteoblasts, we deleted Cx43 exclusively from osteocytes. Mice expressing $Cx43^{fl/fl}$ were crossed with mice expressing the Cre recombinase under the control of an 8kb fragment of the DMP1 promoter (DMP1-8kb-Cre mice). Previous studies demonstrated that several transgenes driven by this fragment of the DMP1 promoter, including GFP, a constitutively active parathyroid hormone receptor 1, and human *SOST*, are expressed in bone and in osteocytes but not in osteoblasts [5,6,29]. Consistent with this earlier evidence, Cre recombinase mRNA was detected only in bone of $Cx43^{\Delta Ot}$ mice, but was absent in brain, kidney, heart, and skeletal muscle in 1-month-old mice (**Fig. 2A**). Cre was undetectable in all these tissues in $Cx43^{fl/fl}$ mice. Moreover, the deleted allele of Cx43 was present at high levels in genomic DNA from bone in $Cx43^{\Delta Ot}$ mice (**Fig. 2B**). Low levels of the deleted allele were also present in brain of $Cx43^{\Delta Ot}$ mice, consistent with a previous study reporting the expression of the DMP1-8kb-GFP transgene in a restricted population of brain cells [29]. Cx43 mRNA levels were not different between control and $Cx43^{\Delta Ot}$ mice in cortical bone preparations likely due to the presence of osteoblasts, as indicated by the expression of keratocan, a gene more abundant in osteoblasts than in osteocytes [44] (**Fig. 2C**). In fact, removal of residual osteoblasts by enzymatic digestion eliminated keratocan expression and revealed that in this osteocyte-enriched cortical bone preparation that express *SOST*, as expected, Cx43 mRNA levels were decreased by about 85% in $Cx43^{\Delta Ot}$ mice compared to littermate controls, demonstrating effective deletion of the gene from osteocytes.

Recent evidence showed that a 10kb fragment of the DMP1 promoter might target the expression of Cre recombinase not only to osteocytes but also to some mature osteoblasts [45,46]. To determine whether the shorter 8kb fragment of the DMP1 promoter used in our studies confers Cre expression exclusively to osteocytes and not to osteoblasts, DMP1-8kb-Cre mice were crossed with DMP1-8kb-GFP mice [29] and neonatal calvaria cells from DMP1-8kb-Cre; DMP1-8Kb-GFP double transgenic mice were subjected to fluorescence activated cell sorting (FACS) to separate GFP positive osteocytes from GFP negative osteoblasts, as previously reported [5]. GFP positive osteocytes (Ot) expressed high

levels of the osteocyte marker *SOST* while keratocan was low, and GFP negative osteoblasts (Ob) had undetectable transcripts for *SOST*, while they expressed higher levels of keratocan (**Fig. 2D**), confirming the identity of the cell populations. Cre recombinase was only detected in GFP positive osteocytes, demonstrating its osteocyte-specific expression. Moreover, Cx43 protein was reduced selectively in osteocytes, but not in osteoblasts, in $Cx43^{\Delta Ot}$ femoral metaphysis, as detected by immunostaining (**Fig. 2E**).

$Cx43^{\Delta Ot}$ mice showed higher total tissue, cortical, and marrow cavity areas, without changes in cortical thickness, resulting in higher minimum moment of inertia (Imin) (**Table 3**). In spite of the increased Imim (**Tables 1** and **3**), bones from $Cx43^{\Delta Ob\text{-}Ot}$ or $Cx43^{\Delta Ot}$ mice did not exhibit increased bone strength (data not show). Similar to mice lacking Cx43 from osteoblasts and osteocytes [(22)], deletion of Cx43 only from osteocytes did not affect bone mass. Total, femoral, and spinal BMD of $Cx43^{fl/fl}$ and $Cx43^{\Delta Ot}$ mice measured by Dexa were similar at 1, 2, 3 and 4 month of age, except for a slight decrease in total BMD at 2 month of age in the $Cx43^{\Delta Ot}$ mice (**Supplementary Fig. 1A**). Bone density measured by μCT (**Table 3**) and femoral length (**Supplementary Fig. 1B**) were also not affected by Cx43 deletion from osteocytes in 4.5-month-old mice (**Table 3**). In cancellous bone, BV/TV, trabecular thickness, number, and separation measured in the femoral metaphysis were not different between the two groups (**Table 4**). Only a small, but significant, increase in circulating osteocalcin and no difference in C-telopeptide were found in $Cx43^{\Delta Ot}$ mice compared to controls (**Supplementary Fig. 1C**). The lack of systemic changes in bone mass and resorption markers is consistent with an effect of Cx43 deletion localized to specific bone compartments. On the other hand, circulating osteocalcin levels were slightly increased, likely as the result of the combination of localized increase in both bone formation and resorption.

## Expression of Cx43 in osteocytes is required to maintain osteocyte viability and to control the RANKL/OPG ratio in a cell autonomous manner

We then investigated whether deletion of Cx43 exclusively from osteocytes lead to similar changes in osteocyte viability than removal of the protein from both osteoblasts and osteocytes. $Cx43^{\Delta Ot}$ mice exhibited a marked increase in the prevalence of osteocyte apoptosis and empty lacunae (**Fig. 3A** and **Supplementary Fig. 2**), suggesting a direct requirement of Cx43 in osteocytes to maintain cell viability. Osteocyte apoptosis has been associated with osteoclast recruitment and localized removal of bone [(7-9,47)]; and targeted death of osteocytes is sufficient to initiate bone resorption [(10)]. Based on this evidence, we next mapped apoptotic osteocytes, empty lacunae, and osteoclasts in different regions of femoral midshaft cross-sections to explore the potential co-localization of these phenomena. Towards this end, the cortex was divided in two equivalent regions: one close to the bone marrow (endocortical, Ec) and the other close to the periosteum (periosteal, Ps); and also in four anatomical regions: anterior, lateral, posterior, and medial (**Fig. 3B**), following earlier approaches [(7,9)]. The accumulation of apoptotic osteocytes was observed in both the periosteal and endocortical halves of the cortex in $Cx43^{\Delta Ot}$ mice compared to controls (**Fig. 3C**). In addition, empty lacunae were uniformly abundant throughout the four anatomical regions of the cortex. In contrast, apoptotic osteocytes were higher in the posterior region of $Cx43^{\Delta Ot}$ mice compared to controls. The prevalence of apoptotic osteocytes among the four regions for either phenotype was not different. Osteoclasts were found only on the endocortical surface and were also more abundant in the posterior region, as well as in the medial region of the cortex (**Fig. 3D**).

Consistent with the lack of systemic changes in resorption, mRNA for RANKL and OPG in whole bones are not different in $Cx43^{\Delta Ot}$ mice compared to controls (not shown). This finding prompted us to investigate potential changes in local gene expression. RANKL and OPG were readily detected by immunostaining in osteocytes in bone sections from $Cx43^{\Delta Ot}$

mice as well as control littermates (**Fig. 3E** and **F** and **Supplementary Fig. 4** and **5**). Moreover, whereas the percentage of osteocytes expressing RANKL was not affected by Cx43 deletion (**Fig. 3E**), the prevalence of OPG-expressing osteocytes was markedly and uniformly reduced in all cortical regions of $Cx43^{\Delta Ot}$ mice (**Fig. 3F**). Similar results were obtained when the prevalence of OPG-expressing osteocytes was calculated by dividing the number of positive cells by the number of total lacunae (**Fig. 3F**) or of occupied lacunae only (**Supplementary Fig. 2B**), indicating that decreased OPG was the result of changes in the expression of the gene and not secondary to the loss of osteocytes. Moreover, the osteocytes showing decreased OPG expression do not appear to correlate with those undergoing apoptosis. Thus, in $Cx43^{\Delta Ot}$ mice, the prevalence of OPG-expressing osteocytes was decreased also in regions in which TUNEL staining of adjacent sections did not show accumulation of apoptotic osteocytes.

To determine whether deletion of Cx43 results in a direct effect on osteocyte viability, we used MLO-Y4 osteocytic cells in which the expression of the protein was silenced using shRNA. Effective deletion of Cx43 was demonstrated at the mRNA and protein level (**Fig. 4B**). Apoptosis was assessed using Trypan blue uptake, a reliable method that correlates with DNA fragmentation, as detected by TUNEL, a recognized hallmark of apoptosis [(48)]. Consistent with the increased osteocyte apoptosis found in $Cx43^{\Delta Ot}$ mice, cultures of MLO-Y4 osteocytic cells in which Cx43 expression was silenced displayed lower number of viable cells due to higher basal levels of apoptosis at 1 to 3 days in culture, compared to MLO-Y4 cells silenced with scrambled shRNA (**Fig. 4A**). On the other hand, proliferation of Cx43 deficient cells, as assessed by BrdU incorporation, did not change throughout the culture period; whereas it declined for Cx43 expressing cells as cultures reached confluence. In addition, RANKL expression was higher and OPG expression was lower in MLO-Y4 cells lacking Cx43 compared to MLO-Y4 cells expressing Cx43, resulting in approximately a 4-fold increase in the RANKL/OPG ratio (**Fig. 4B**). Similar results were obtained with primary cultures of calvaria cells derived from $Cx43^{\Delta Ot}$ mice (**Fig. 4C**). Taken together, these results indicate that Cx43 is required in a cell autonomous manner to maintain osteocyte viability and to regulate the RANKL/OPG ratio.

## Increased periosteal bone apposition and endocortical bone formation in $Cx43^{\Delta Ot}$ mice is localized in areas of low sclerostin levels due to loss of viable osteocytes

The larger femora cross-section displayed by $Cx43^{\Delta Ot}$ mice was associated with increased periosteal bone apposition, as demonstrated by increased BFR/BS, MAR and MS/BS (**Fig. 5A**). Similar to our findings with osteoclast surface, periosteal bone formation was selectively activated in defined portions of the cortex. Thus, BFR/BS was increased in the posterior and medial periosteal surfaces in $Cx43^{\Delta Ot}$ femora, resulting from higher MAR. Consistent with the role of sclerostin as a paracrine inhibitor of bone formation [(2,49)], the percentage of osteocytes expressing sclerostin was significantly reduced in the periosteal half of the femoral cortex in $Cx43^{\Delta Ot}$ mice. Moreover, sclerostin-expressing osteocytes were reduced in the posterior and medial regions of the periosteal half, areas in which bone formation was increased, as well as in the anterior region (**Fig. 5A** and **Supplementary Fig. 6**). Bone formation was also enhanced on the endocortical surface and it was localized to the anterior portion of the cortex, where the prevalence of sclerostin-positive osteocytes per total lacunae was decreased (**Fig. 5B**). In contrast to OPG-expressing osteocytes, the decrease in the prevalence of sclerostin-expressing osteocytes was eliminated when the number of positive cells was divided by the number of occupied lacunae (**Supplementary Fig. 2C**), suggesting that deletion of Cx43 does not reduce *SOST* expression in individual osteocytes. We confirmed that changes in Cx43 levels do not affect *SOST* expression *in vitro* by comparing the expression of the gene in UMR-106 cells, which exhibit low Cx43 expression, and UMR-43 cells, a cell line derived from UMR-106 cells that overexpresses

Cx43 [16]. In contrast to MLO-Y4 cells, which do not express *SOST* transcripts, UMR-106 cells express high levels of *SOST* and low levels of Cx43 that can be increased by stable transfection [16,50,51]. Even when Cx43 expression was significantly lower in UMR-106 wild type cells compared to UMR-43 cells, both cell types expressed similar *SOST* levels (**Fig. 4D**). Thus, this *in vivo* and *in vitro* evidence strongly suggest that whereas decreased OPG expression is due to an intrinsic reduction in gene expression, decreased sclerostin levels result from loss of viable osteocytes in $Cx43^{\Delta Ot}$ mice.

## DISCUSSION

The findings of the present study demonstrate conclusively that Cx43 is required in a cell autonomous fashion to preserve the viability of osteocytes and to control in osteocytes the levels of proteins that regulate the generation and activity of osteoclasts and osteoblasts. Cx43 deficiency causes an intrinsic reduction in OPG expression and loss of viable osteocytes, with the consequent decrease in local levels of the bone formation inhibitor sclerostin. Our results indicate that there is a potential cause-effect relationship between these molecular events and the exacerbated endocortical resorption and periosteal bone formation in selected areas of the cortex, which alter bone geometry (**Fig. 6**). Bone formation and resorption triggered by Cx43 removal occur on separate, non-overlapping locations within cortical bone, suggesting that the two events are not coupled during bone remodeling, and that instead the absence of Cx43 enhances formation and resorption due to modeling. Remarkably, the bone surfaces that show increased activity in the Cx43 conditional knock-out mice are the same ones that are subjected to modeling during growth [52], suggesting the potential involvement of osteocytes and Cx43 in this physiological process. In addition, $Cx43^{\Delta Ob\text{-}Ot/-}$ and $Cx43^{\Delta Ot}$ mice display features that resemble bones from aging rodents and humans, including accumulation of apoptotic osteocytes and empty lacunae and periosteal expansion of the long bones [41,53]. Because Cx43 is a Wnt target gene [54] and Wnt signaling decreases with age in bone [55], our findings raise the possibility that reduction in Cx43 expression due to decreased Wnt signaling could mediate at least some of the changes induced by aging in the skeleton.

Previous reports have shown that deletion of Cx43 from osteochondroprogenitors or from early osteoblast progenitors, or the disruption of its function by expressing a oculodentodigital dysplasia-like Cx43 mutant, result in reduced bone mass due to deficient osteoblast differentiation and function [19,20,56-58]. However, deletion of Cx43 from mature osteoblasts and osteocytes [22] or from osteocytes only (this report), does not cause a decrease in bone mass, indicating that Cx43 is specifically required for osteoblast maturation during early stages of differentiation and its removal from cells at a more mature osteoblastic stage does not affect bone mass. On the other hand, the widening of the long bones, a phenotypic feature present in the mouse models of early Cx43 deletion, was reproduced in $Cx43^{\Delta Ot}$ mice. This indicates that the removal of Cx43 from osteocytes is sufficient to elicit the changes in the geometry typical of Cx43 deletion and further supports the notion that Cx43 expression specifically in osteocytes is required to regulate bone modeling in cortical bone.

The decrease in osteocalcin levels in $Cx43^{\Delta Ob\text{-}Ot/-}$ mice is likely the systemic expression of a generalized reduction in osteoblast activity due to Cx43 removal from osteoblasts. Indeed, it was previously shown that Cx43-deficient osteoblasts express low levels of osteocalcin [20,42]. On the other hand, deletion of Cx43 from osteoblasts and osteocytes enhances the bone-forming activity of periosteal cells, as shown by us and others [19], suggesting that the activity of cells on the periosteal and endocortical surfaces is regulated by different mechanism. Consistent with this, deletion of Cx43 only from osteocytes in $Cx43^{\Delta Ot}$ mice results in a significantly higher circulating osteocalcin level, likely resulting

from the enhanced osteoblastic activity in both endocortical and periosteal surfaces and lack of impairment of osteoblast function in other surfaces. Moreover, our studies raise the possibility that osteocytes and osteocyte apoptosis are novel players in the establishment of geometrical phenotype caused by ODDD-related mutations.

Our study is the first one to demonstrate that lack of Cx43 in osteocytes leads to their apoptosis. These findings are consistent with earlier studies of ours in which Cx43 was shown to act as a transducer of cell survival signals generated by bisphosphonates in osteoblasts and osteocytes [16,22]. Our current study raises the possibility that physiological pro-survival signals for osteocytes are also transduced by Cx43, although the identity of the endogenous stimuli that protect osteocytes from apoptosis is not known. Similar to lack of Cx43, weightlessness induced by unloading *in vivo* in rodents or *in vitro* in human explants, increases the prevalence of osteocyte apoptosis [7,59-61]. Conversely, mechanical stimulation prevents apoptosis of osteocytic cells [62,63], and induces opening of Cx43 hemichannels [64], which in turn is required for the release of prostaglandins and preservation of cell survival [65]. Taken together this evidence suggests that mechanical forces might require Cx43 to maintain osteocyte viability. Local factors present in the bone microenvironment might also activate Cx43-dependent signaling. A potential candidate is IGF-I, which prevents apoptosis of osteoblastic cells *in vitro* and increases the percentage of occupied osteocyte lacunae *in vivo* [66,67], by a mechanism that might require Cx43, as shown for cardiomyocyte progenitor cells [68]. Similar to our findings demonstrating that lack of Cx43 leads to apoptosis of osteocytes but not of osteoblasts, mechanical stimulation and IGF-I appear to differentially affect survival of these two cell types. Thus, osteoblasts and osteocytes exhibit different sensitivity to mechanical forces *in vitro* [69,70]; and, whereas osteocytic cells open Cx43 hemichannels in response to mechanical stimulation, osteoblastic cells do not [71]. In addition, mice overexpressing IGF-I in osteoblastic cells do not exhibit changes in osteoblast viability, while they appear to display prolonged osteocyte survival [67]. Future studies will be required to identify physiologic cues that require Cx43 to maintain osteocyte viability.

The intracellular survival events activated downstream of Cx43 under physiological conditions also remain unknown. We have shown that the Cx43-dependent survival effect of bisphosphonates on osteocytes is mediated by activation of Src and the survival kinases ERKs [16]. In addition, osteoblastic cells with deficient Cx43 function exhibit reduced ERK activation in response to growth factors [72]. Moreover, mechanical stimulation, systemic hormones, as well as local factors such as Wnts and IGF-I, all known ERK-activating stimuli, prevent apoptosis of osteoblastic cells [73]. Whether alterations in the ERK pathway are responsible for increased osteocyte apoptosis in the absence of Cx43 will require future investigations.

Our studies show apoptotic osteocytes only in cortical bone but not in cancellous bone of mice with conditional deletion of Cx43. In addition, Cx43 protein expression appears to be higher in the cortical envelope, compared to the cancellous compartment in control mice (not shown), consistent with recent evidence suggesting higher expression of Cx43 in osteocytes in cortical versus cancellous bone [19]. This differential expression raises the possibility that higher levels of Cx43 are required to maintain viability of osteocytes in cortical bone, compared to cancellous bone. In addition, intrinsic differences in threshold sensitivity to environmental cues between cells in these two bone envelopes could explain this phenomenon. Alternatively, the failure to detect increases in the prevalence of osteocyte apoptosis in cancellous bone could be explained by the higher rate of remodeling in this compartment compared to cortical bone, which would not allow accumulation of apoptotic osteocytes. Consistent with this hypothesis, we have shown in a previous study that inhibition of resorption by alendronate administration to $Cx43^{\Delta Ob\text{-}Ot/-}$ mice led to a

significant increase in the prevalence of osteocyte apoptosis in vertebral cancellous bone, reaching values close to those observed in cortical bone [22]. Thus, apoptotic osteocytes might accumulate as the animals age as a result of the decreased rate of bone remodeling [53], suggesting that a cancellous bone phenotype could become evident in older mice.

The association between osteocyte apoptosis and increased osteoclasts on adjacent endocortical surfaces in $Cx43^{\Delta Ot}$ mice is consistent with previous evidence suggesting that dying osteocytes recruit osteoclasts to the vicinity [11]. Blockade of osteocyte apoptosis with caspase inhibitors prevented the expected increase in bone resorption induced by fatigue loading or ovariectomy [8,9]. However, the mechanism of this osteocyte-induced osteoclast recruitment is not known. In an attempt to identify molecules produced by osteocytes that could induce local resorption, we mapped the number and distribution of osteocytes expressing RANKL and OPG, molecules shown to be expressed by osteocytes [3,4]. To do this, we performed immunohistochemistry staining of bone sections using specific antibodies directed against RANKL and OPG. Although not quantitative, this approach is ideal to show the expression of RANKL and OPG in osteocytes and the spatial distribution of the two proteins in relation to osteoclasts. Expression of RANKL and OPG mRNA and protein was readily detected in bone lysates or sections, respectively, although no differences were detected in bone lysates from $Cx43^{\Delta Ot}$ mice compared to wild type littermates (not shown). Moreover, the percent of RANKL positive osteocytes was similar between the two mouse strains. On the other hand, the number of osteocytes expressing OPG was markedly reduced in conditional knock-out mice. This is similar to the recent findings in mice lacking Cx43 in osteochondroprogenitors, which also exhibit an increased RANKL/OPG ratio due to reduced levels of OPG [19], strongly suggesting that removal of Cx43 from osteocytes is responsible for the changes observed in the later mouse model. However, in our $Cx43^{\Delta Ot}$ model osteocytes expressing low levels of OPG were equally distributed throughout the cortex, suggesting that an increase in RANKL/OPG ratio is not sufficient to increase resorption and that additional signals are required to target osteoclasts to particular areas of the bone. Empty osteocyte lacunae were also evenly distributed throughout the cortical bone, arguing against the possibility that osteoclast recruitment results from loss of osteoclast-restraining signals released by living osteocytes, as previously suggested [74]. In contrast, we found that apoptotic osteocytes were located nearby osteoclasts, supporting the notion that during the process of undergoing apoptosis, osteocytes actively emit signals that promote recruitment and differentiation of osteoclast progenitors [75]. This is consistent with previous reports showing that dying osteocytes release apoptotic bodies, which induce osteoclast differentiation [47]. Indeed, we observed TUNEL positivity not only in osteocytic cell bodies but also within canaliculi, suggesting that fragmented DNA and potentially other components of dying cells escape to the canalicular network. These chemotactic signals could be, in turn, transported through the canaliculi to regions adjacent to the ones in which they were produced. This could explain our finding that osteoclast number is also higher in the medial region, in the absence of increased osteocyte apoptosis in the same area. Taken together with previous evidence, our findings suggest that, reduced OPG expression may be a permissive event, and that signaling molecules derived from dying osteocytes, may act as chemo-attractants for osteoclast precursors to trigger bone resorption at specific locations.

Reduced percentage of OPG-expressing osteocytes was found independently of whether OPG-expressing cells were divided by total number of lacunae or by occupied lacunae only, thus indicating that reduction in OPG is not a consequence of loss of viable osteocytes. This, together with the findings that OPG mRNA expression is decreased in cultured MLO-Y4 cells lacking Cx43, confirms a cell autonomous regulation of OPG by Cx43 and raises the possibility that Cx43 directly controls the transcription of OPG. Expression of both Cx43

and OPG is increased by Wnt signaling [4,54]. Our findings showing that mice lacking Cx43 in osteocytes exhibit low OPG expression raise the possibility that Wnt signaling upregulates OPG by a mechanism that involves Cx43. Besides containing consensus Lef1/Tcf binding sequences through which the Wnt pathway directly increases gene expression [76], the OPG promoter also displays binding sites for Sp1 and p53 [77,78], transcription factors known to be regulated by Cx43 [18,79]. Thus, it is possible that these Cx43-dependent transcription factors interact with Wnt/βcatenin to enhance transcriptional activation of the OPG gene, similar to what it was proposed for BMPs [76]. On the other hand, Cx43 does not appear to directly promote the transcription of *SOST*/sclerostin, since overexpression of Cx43 in UMR-106 cells does not affect mRNA levels for *SOST*. In contrast to OPG, the percentage of RANKL positive osteocytes is not different in $Cx43^{\Delta Ot}$ mice. However, it is possible that each osteocyte expresses more RANKL, which cannot be quantified by immunohistochemistry. Indeed, MLO-Y4 cells lacking Cx43 do express more RANKL. Thus, we cannot exclude the possibility that increased RANKL expression in selected osteocyte populations contributes to increased local RANKL/OPG ratio and resorption *in vivo*.

We conclude that Cx43 is differentially required for maintaining osteocyte viability in cortical but not cancellous bone in a cell autonomous manner. Deletion of Cx43 from osteocytes also alters gene expression and bone formation and resorption, which result in changes in bone geometry. Whether these effects of Cx43 result from the ability of the protein to mediate osteocyte communication with other cells or with the extracellular milieu or are due to its interaction with signaling molecules resulting in modulation of intracellular pathways will require further investigation.

## Supplementary Material

Refer to Web version on PubMed Central for supplementary material.

## Acknowledgments

The authors thank Thomas R. Murphy, Kanan Vyas, Jeffrey Benson, Racheal Lee, Logan Vaught, and Caroline Miller for technical assistance, Charles Turner and Vincent Gattone III for insightful suggestions, and Dr. David Burr for the critical reading of the manuscript. This research was supported by the National Institutes of Health (R01-AR053643 to LP; KO2-AR02127, R03 TW006919, R01-DK076007, and P01-AG13918 to TB; and RR025761 to the Indiana Clinical and Translational Sciences Institute at Indiana University). μCT studies were performed using equipment obtained with the NIH grant S10-RR023710 (PI: James Williams, Department of Anatomy and Cell Biology, Indiana University School of Medicine).

## REFERENCES

1. Klein-Nulend, J.; Bonewald, LF. The osteocyte.. In: Bilezikian, JP.; Raisz, LG.; Martin, TJ., editors. Principles of Bone Biology. Third ed.. Academic Press; San Diego, CA: 2008. p. 153-174.
2. Paszty C, Turner CH, Robinson MK. Sclerostin: a gem from the genome leads to bone-building antibodies. J Bone Miner Res. 2010; 25:1897–1904. [PubMed: 20564241]
3. Zhao S, Zhang YK, Harris S, Ahuja SS, Bonewald LF. MLO-Y4 osteocyte-like cells support osteoclast formation and activation. J Bone Miner Res. 2002; 17:2068–2079. [PubMed: 12412815]
4. Kramer I, Halleux C, Keller H, Pegurri M, Gooi JH, Weber PB, Feng JQ, Bonewald LF, Kneissel M. Osteocyte Wnt/beta-catenin signaling is required for normal bone homeostasis. Mol Cell Biol. 2010; 30:3071–3085. [PubMed: 20404086]
5. O'Brien CA, Plotkin LI, Galli C, Goellner J, Gortazar AR, Allen MR, Robling AG, Bouxsein M, Schipani E, Turner CH, Jilka RL, Weinstein RS, Manolagas SC, Bellido T. Control of bone mass and remodeling by PTH receptor signaling in osteocytes. PLoS ONE. 2008; 3:e2942. [PubMed: 18698360]

6. Rhee Y, Allen MR, Condon K, Lezcano V, Ronda AC, Galli C, Olivos N, Passeri G, O'Brien CA, Bivi N, Plotkin LI, Bellido T. PTH receptor signaling in osteocytes governs periosteal bone formation and intra-cortical remodeling. J Bone Miner Res. 2011; 26:1035–1046. [PubMed: 21140374]
7. Aguirre JI, Plotkin LI, Stewart SA, Weinstein RS, Parfitt AM, Manolagas SC, Bellido T. Osteocyte apoptosis is induced by weightlessness in mice and precedes osteoclast recruitment and bone loss. J Bone Min Res. 2006; 21:605–615.
8. Cardoso L, Herman BC, Verborgt O, Laudier D, Majeska RJ, Schaffler MB. Osteocyte apoptosis controls activation of intracortical resorption in response to bone fatigue. J Bone Miner Res. 2009; 24:597–605. [PubMed: 19049324]
9. Emerton KB, Hu B, Woo AA, Sinofsky A, Hernandez C, Majeska RJ, Jepsen KJ, Schaffler MB. Osteocyte apoptosis and control of bone resorption following ovariectomy in mice. Bone. 2009; 46:577–583. [PubMed: 19925896]
10. Tatsumi S, Ishii K, Amizuka N, Li M, Kobayashi T, Kohno K, Ito M, Takeshita S, Ikeda K. Targeted ablation of osteocytes induces osteoporosis with defective mechanotransduction. Cell Metab. 2007; 5:464–475. [PubMed: 17550781]
11. Bellido T. Osteocyte apoptosis induce bone resorption and impairs the skeletal response to weightlessness. BoneKEy-osteovision. 2007; 4:252–256.
12. Civitelli R. Cell-cell communication in the osteoblast/osteocyte lineage. Arch Biochem Biophys. 2008; 473:188–192. [PubMed: 18424255]
13. Goodenough DA, Paul DL. Beyond the gap: functions of unpaired connexon channels. Nat Rev Mol Cell Biol. 2003; 4:285–294. [PubMed: 12671651]
14. Giepmans BN. Gap junctions and connexin-interacting proteins. Cardiovasc Res. 2004; 62:233–245. [PubMed: 15094344]
15. Plotkin LI, Weinstein RS, Parfitt AM, Roberson PK, Manolagas SC, Bellido T. Prevention of osteocyte and osteoblast apoptosis by bisphosphonates and calcitonin. J Clin Invest. 1999; 104:1363–1374. [PubMed: 10562298]
16. Plotkin LI, Manolagas SC, Bellido T. Transduction of cell survival signals by connexin-43 hemichannels. J Biol Chem. 2002; 277:8648–8657. [PubMed: 11741942]
17. Bivi N, Lezcano V, Romanello M, Bellido T, Plotkin LI. Connexin43 interacts with βarrestin: a pre-requisite for osteoblast survival induced by parathyroid hormone. J Cell Biochem. 2011 DOI 10.1002/jcb.23208.
18. Stains JP, Lecanda F, Screen J, Towler DA, Civitelli R. Gap junctional communication modulates gene transcription by altering the recruitment of Sp1 and Sp3 to connexin - response elements in osteoblast promoters. J Biol Chem. 2003; 278:24377–24387. [PubMed: 12700237]
19. Watkins M, Grimston SK, Norris JY, Guillotin B, Shaw A, Beniash E, Civitelli R. Osteoblast Connexin43 modulates skeletal architecture by regulating both arms of bone remodeling. Mol Biol Cell. 2011; 22:1240–1251. [PubMed: 21346198]
20. Chung D, Castro CH, Watkins M, Stains JP, Chung MY, Szejnfeld VL, Willecke K, Theis M, Civitelli R. Low peak bone mass and attenuated anabolic response to parathyroid hormone in mice with an osteoblast-specific deletion of connexin43. J Cell Sci. 2006; 119:4187–4198. [PubMed: 16984976]
21. Paznekas WA, Boyadjiev SA, Shapiro RE, Daniels O, Wollnik B, Keegan CE, Innis JW, Dinulos MB, Christian C, Hannibal MC, Jabs EW. Connexin 43 (GJA1) mutations cause the pleiotropic phenotype of oculodentodigital dysplasia. Am J Hum Genet. 2002; 72:408–418. [PubMed: 12457340]
22. Plotkin LI, Lezcano V, Thostenson J, Weinstein RS, Manolagas SC, Bellido T. Connexin 43 is required for the anti-apoptotic effect of bisphosphonates on osteocytes and osteoblasts in vivo. J Bone Miner Res. 2008; 23:1712–1721. [PubMed: 18597631]
23. Lakso M, Sauer B, Mosinger B Jr. Lee EJ, Manning RW, Yu SH, Mulder KL, Westphal H. Targeted oncogene activation by site-specific recombination in transgenic mice. Proc Natl Acad Sci U S A. 1992; 89:6232–6236. [PubMed: 1631115]
24. Orban PC, Chui D, Marth JD. Tissue- and site-specific DNA recombination in transgenic mice. Proc Natl Acad Sci U S A. 1992; 89:6861–6865. [PubMed: 1495975]

25. Theis M, de Wit C, Schlaeger TM, Eckardt D, Kruger O, Doring B, Risau W, Deutsch U, Pohl U, Willecke K. Endothelium-specific replacement of the connexin43 coding region by a lacZ reporter gene. Genesis. 2001; 29:1–13. [PubMed: 11135457]
26. Reaume AG, de Sousa PA, Kulkarni S, Langille BL, Zhu D, Davies TC, Juneja SC, Kidder GM, Rossant J. Cardiac malformation in neonatal mice lacking connexin43. Science. 1995; 267:1831–1834. [PubMed: 7892609]
27. Zhang M, Xuan S, Bouxsein ML, Von Stechow D, Akeno N, Faugere MC, Malluche H, Zhao G, Rosen CJ, Efstratiadis A, Clemens TL. Osteoblast-specific knockout of the insulin-like growth factor (IGF) receptor gene reveals an essential role of IGF signaling in bone matrix mineralization. J Biol Chem. 2002; 277:44005–44012. [PubMed: 12215457]
28. Calera MR, Wang Z, Sanchez-Olea R, Paul DL, Civan MM, Goodenough DA. Depression of intraocular pressure following inactivation of connexin43 in the nonpigmented epithelium of the ciliary body. Invest Ophthalmol Vis Sci. 2009; 50:2185–2193. [PubMed: 19168903]
29. Kalajzic I, Braut A, Guo D, Jiang X, Kronenberg MS, Mina M, Harris MA, Harris SE, Rowe DW. Dentin matrix protein 1 expression during osteoblastic differentiation, generation of an osteocyte GFP-transgene. Bone. 2004; 35:74–82. [PubMed: 15207743]
30. Silverstein DM, Urban M, Gao Y, Mattoo TK, Spray DC, Rozental R. Renal morphology in connexin43 knockout mice. Pediatr Nephrol. 2001; 16:467–471. [PubMed: 11420908]
31. Hilton MJ, Tu X, Wu X, Bai S, Zhao H, Kobayashi T, Kronenberg HM, Teitelbaum SL, Ross FP, Kopan R, Long F. Notch signaling maintains bone marrow mesenchymal progenitors by suppressing osteoblast differentiation. Nat Med. 2008; 14:306–314. [PubMed: 18297083]
32. Allen MR, Reinwald S, Burr DB. Alendronate reduces bone toughness of ribs without significantly increasing microdamage accumulation in dogs following 3 years of daily treatment. Calcif Tissue Int. 2008; 82:354–360. [PubMed: 18463913]
33. Plotkin LI, Bivi N, Bellido T. A bisphosphonate that does not affect osteoclasts prevents osteoblast and osteocyte apoptosis and the loss of bone strength induced by glucocorticoids in mice. Bone. 2011; 49:122–127. [PubMed: 20736091]
34. Hauge E, Mosekilde L, Melsen F. Missing observations in bone histomorphometry on osteoporosis: implications and suggestions for an approach. Bone. 1999; 25:389–395. [PubMed: 10511104]
35. Parfitt AM, Drezner MK, Glorieux FH, Kanis JA, Malluche H, Meunier PJ, Ott SM, Recker RR. Bone histomorphometry: standardization of nomenclature, symbols, and units. J Bone Min Res. 1987; 2:595–610.
36. Rhee Y, Bivi N, Farrow EG, Lezcano V, Plotkin LI, White KE, Bellido T. Parathyroid hormone receptor signaling in osteocytes increases the expression of fibroblast growth factor-23 *in vitro* and *in vivo*. Bone. 2011 doi:10.1016/j.bone.2011.06.025.
37. Bellido T, Ali AA, Plotkin LI, Fu Q, Gubrij I, Roberson PK, Weinstein RS, O'Brien CA, Manolagas SC, Jilka RL. Proteasomal degradation of Runx2 shortens parathyroid hormone-induced anti-apoptotic signaling in osteoblasts. A putative explanation for why intermittent administration is needed for bone anabolism. J Biol Chem. 2003; 278:50259–50272. [PubMed: 14523023]
38. Erlebacher A, Derynck R. Increased expression of TGF-beta 2 in osteoblasts results in an osteoporosis-like phenotype. J Cell Biol. 1996; 132:195–210. [PubMed: 8567723]
39. Bivi N, Bereszczak JZ, Romanello M, Zeef LA, Delneri D, Quadrifoglio F, Moro L, Brancia FL, Tell G. Transcriptome and proteome analysis of osteocytes treated with nitrogen-containing bisphosphonates. J Proteome Res. 2009; 8:1131–1142. [PubMed: 19226166]
40. Riffenburgh, RH. Statistics in Medicine. 2nd ed.. Academic Press; 2006.
41. Qiu S, Rao DS, Palnitkar S, Parfitt AM. Age and distance from the surface but not menopause reduce osteocyte density in human cancellous bone. Bone. 2002; 31:313–318. [PubMed: 12151084]
42. Lecanda F, Warlow PM, Sheikh S, Furlan F, Steinberg TH, Civitelli R. Connexin43 deficiency causes delayed ossification, craniofacial abnormalities, and osteoblast dysfunction. J Cell Biol. 2000; 151:931–944. [PubMed: 11076975]

43. Weinstein RS, Roberson PK, Manolagas SC. Giant osteoclast formation and long-term oral bisphosphonate therapy. N Engl J Med. 2009; 360:53–62. [PubMed: 19118304]
44. Paic F, Igwe JC, Nori R, Kronenberg MS, Franceschetti T, Harrington P, Kuo L, Shin DG, Rowe DW, Harris SE, Kalajzic I. Identification of differentially expressed genes between osteoblasts and osteocytes. Bone. 2009; 45:682–692. [PubMed: 19539797]
45. Xiao Z, Dallas M, Qiu N, Nicolella D, Cao L, Johnson M, Bonewald L, Quarles LD. Conditional deletion of Pkd1 in osteocytes disrupts skeletal mechanosensing in mice. FASEB J. 2011; 25:2418–2432. [PubMed: 21454365]
46. Lu Y, Xie Y, Zhang S, Dusevich V, Bonewald LF, Feng JQ. DMP1-targeted Cre expression in odontoblasts and osteocytes. J Dent Res. 2007; 86:320–325. [PubMed: 17384025]
47. Kogianni G, Mann V, Noble BS. Apoptotic bodies convey activity capable of initiating osteoclastogenesis and localised bone destruction. J Bone Miner Res. 2008; 23:915–927. [PubMed: 18435576]
48. Bellido, T.; Plotkin, LI. Detection of apoptosis of bone cells in vitro.. In: Westendorf, JJ., editor. Osteoporosis. Humana Press; 2007. p. 51-75.
49. Robling AG, Niziolek PJ, Baldridge LA, Condon KW, Allen MJ, Alam I, Mantila SM, Gluhak-Heinrich J, Bellido T, Harris SE, Turner CH. Mechanical stimulation of bone in vivo reduces osteocyte expression of Sost/sclerostin. J Biol Chem. 2008; 283:5866–5875. [PubMed: 18089564]
50. Bellido T, Ali AA, Gubrij I, Plotkin LI, Fu Q, O'Brien CA, Manolagas SC, Jilka RL. Chronic elevation of PTH in mice reduces expression of sclerostin by osteocytes: a novel mechanism for hormonal control of osteoblastogenesis. Endocrinology. 2005; 146:4577–4583. [PubMed: 16081646]
51. Keller H, Kneissel M. SOST is a target gene for PTH in bone. Bone. 2005; 37:148–158. [PubMed: 15946907]
52. Frost HM. Strain and other mechanical influences on bone strength and maintenance. Curr Opin Orthop. 1997; 8:60–70.
53. Almeida M, Han L, Martin-Millan M, Plotkin LI, Stewart SA, Roberson PK, Kousteni S, O'Brien CA, Bellido T, Parfitt AM, Weinstein RS, Jilka RL, Manolagas SC. Skeletal involution by age-associated oxidative stress and its acceleration by loss of sex steroids. J Biol Chem. 2007; 282:27285–27297. [PubMed: 17623659]
54. Robinson JA, Chatterjee-Kishore M, Yaworsky PJ, Cullen DM, Zhao W, Li C, Kharode Y, Sauter L, Babij P, Brown EL, Hill AA, Akhter MP, Johnson ML, Recker RR, Komm BS, Bex FJ. WNT/beta-catenin signaling is a normal physiological response to mechanical loading in bone. J Biol Chem. 2006; 281:31720–31728. [PubMed: 16908522]
55. Almeida M, Han L, Martin-Millan M, O'Brien CA, Manolagas SC. Oxidative stress antagonizes Wnt signaling in osteoblast precursors by diverting beta-catenin from T cell factor- to forkhead box O-mediated transcription. J Biol Chem. 2007; 282:27298–27305. [PubMed: 17623658]
56. Grimston SK, Brodt MD, Silva MJ, Civitelli R. Attenuated response to in vivo mechanical loading in mice with conditional osteoblast ablation of the Connexin43 gene (Gja1). J Bone Miner Res. 2008; 23:879–886. [PubMed: 18282131]
57. Dobrowolski R, Sasse P, Schrickel JW, Watkins M, Kim JS, Rackauskas M, Troatz C, Ghanem A, Tiemann K, Degen J, Bukauskas FF, Civitelli R, Lewalter T, Fleischmann BK, Willecke K. The conditional connexin43G138R mouse mutant represents a new model of hereditary oculodentodigital dysplasia in humans. Hum Mol Genet. 2008; 17:539–554. [PubMed: 18003637]
58. Zhang Y, Paul EM, Donahue HJ. Connexin 43 and osteocyte regulation of osteoclastogenesis and bone resorption. J Bone Miner Res. 2009; 24:S13.
59. Dufour C, Holy X, Marie PJ. Skeletal unloading induces osteoblast apoptosis and targets alpha5beta1-PI3K-Bcl-2 signaling in rat bone. Exp Cell Res. 2007; 313:394–403. [PubMed: 17123509]
60. Basso N, Heersche JN. Effects of hind limb unloading and reloading on nitric oxide synthase expression and apoptosis of osteocytes and chondrocytes. Bone. 2006; 39:807–814. [PubMed: 16765658]

61. Mann V, Huber C, Kogianni G, Jones D, Noble B. The influence of mechanical stimulation on osteocyte apoptosis and bone viability in human trabecular bone. J Musculoskelet Neuronal Interact. 2006; 6:408–417. [PubMed: 17185839]
62. Bakker A, Klein-Nulend J, Burger E. Shear stress inhibits while disuse promotes osteocyte apoptosis. Biochem Biophys Res Commun. 2004; 320:1163–1168. [PubMed: 15249211]
63. Plotkin LI, Mathov I, Aguirre JI, Parfitt AM, Manolagas SC, Bellido T. Mechanical stimulation prevents osteocyte apoptosis: requirement of integrins, Src kinases and ERKs. Am J Physiol Cell Physiol. 2005; 289:C633–C643. [PubMed: 15872009]
64. Cherian PP, Siller-Jackson AJ, Gu S, Wang X, Bonewald LF, Sprague E, Jiang JX. Mechanical strain opens connexin 43 hemichannels in osteocytes: a novel mechanism for the release of prostaglandin. Mol Biol Cell. 2005; 16:3100–3106. [PubMed: 15843434]
65. Kitase Y, Barragan L, Jiang JX, Johnson ML, Bonewald LF. Mechanical induction of PGE(2) in osteocytes blocks glucocorticoid induced apoptosis through both the beta-catenin and PKA pathways. J Bone Miner Res. 2010; 25:2381–2392.
66. Hill PA, Tumber A, Meikle MC. Multiple extracellular signals promote osteoblast survival and apoptosis. Endocrinology. 1997; 138:3849–3858. [PubMed: 9275074]
67. Zhao G, Monier-Faugere MC, Langub MC, Geng Z, Nakayama T, Pike JW, Chernausek SD, Rosen CJ, Donahue LR, Malluche HH, Fagin JA, Clemens TL. Targeted overexpression of insulin-like growth factor I to osteoblasts of transgenic mice: increased trabecular bone volume without increased osteoblast proliferation. Endocrinology. 2000; 141:2674–2682. [PubMed: 10875273]
68. Lu G, Haider HK, Jiang S, Ashraf M. Sca-1+ stem cell survival and engraftment in the infarcted heart: dual role for preconditioning-induced connexin-43. Circulation. 2009; 119:2587–2596. [PubMed: 19414636]
69. Aguirre JI, Plotkin LI, Gortazar AR, O'Brien CA, Manolagas SC, Bellido T. A novel ligand-independent function of the estrogen receptor is essential for osteocyte and osteoblast mechanotransduction. J Biol Chem. 2007; 282:25501–25508. [PubMed: 17609204]
70. Ponik SM, Triplett JW, Pavalko FM. Osteoblasts and osteocytes respond differently to oscillatory and unidirectional fluid flow profiles. J Cell Biochem. 2007; 100:794–807. [PubMed: 17031855]
71. Genetos DC, Kephart CJ, Zhang Y, Yellowley CE, Donahue HJ. Oscillating fluid flow activation of gap junction hemichannels induces ATP release from MLO-Y4 osteocytes. J Cell Physiol. 2007; 212:207–214. [PubMed: 17301958]
72. Stains JP, Civitelli R. Gap junctions regulate extracellular signal-regulated kinase signaling to affect gene transcription. Mol Biol Cell. 2005; 16:64–72. [PubMed: 15525679]
73. Jilka, RL.; Bellido, T.; Almeida, M.; Plotkin, LI.; O'Brien, CA.; Weinstein, RS.; Manolagas, SC. Apoptosis in bone cells.. In: Bilezikian, JP.; Raisz, LG.; Martin, TJ., editors. Principles of Bone Biology. 3er ed.. Academic Press; San Diego, San Francisco, New York, London, Sydney, Tokyo: 2008. p. 237-261.
74. Gu G, Mulari M, Peng Z, Hentunen TA, Vaananen HK. Death of osteocytes turns off the inhibition of osteoclasts and triggers local bone resorption. Biochem Biophys Res Commun. 2005; 335:1095–1101. [PubMed: 16111656]
75. Noble BS, Peet N, Stevens HY, Brabbs A, Mosley JR, Reilly GC, Reeve J, Skerry TM, Lanyon LE. Mechanical loading: biphasic osteocyte survival and the targeting of osteoclasts for bone destruction in rat cortical bone. Am J Physiol Cell Physiol. 2003; 284:C934–C943. [PubMed: 12477665]
76. Sato MM, Nakashima A, Nashimoto M, Yawaka Y, Tamura M. Bone morphogenetic protein-2 enhances Wnt/beta-catenin signaling-induced osteoprotegerin expression. Genes Cells. 2009; 14:141–153. [PubMed: 19170762]
77. Subramaniam M, Hawse JR, Bruinsma ES, Grygo SB, Cicek M, Oursler MJ, Spelsberg TC. TGFbeta inducible early gene-1 directly binds to, and represses, the OPG promoter in osteoblasts. Biochem Biophys Res Commun. 2010; 392:72–76. [PubMed: 20059964]
78. Secchiero P, Corallini F, Rimondi E, Chiaruttini C, di Lasio MG, Rustighi A, Del Sal G, Zauli G. Activation of the p53 pathway down-regulates the osteoprotegerin expression and release by vascular endothelial cells. Blood. 2008; 111:1287–1294. [PubMed: 18000166]

79. Francis RJ, Lo CW. Primordial germ cell deficiency in the connexin 43 knockout mouse arises from apoptosis associated with abnormal p53 activation. Development. 2006; 133:3451–3460. [PubMed: 16887824]

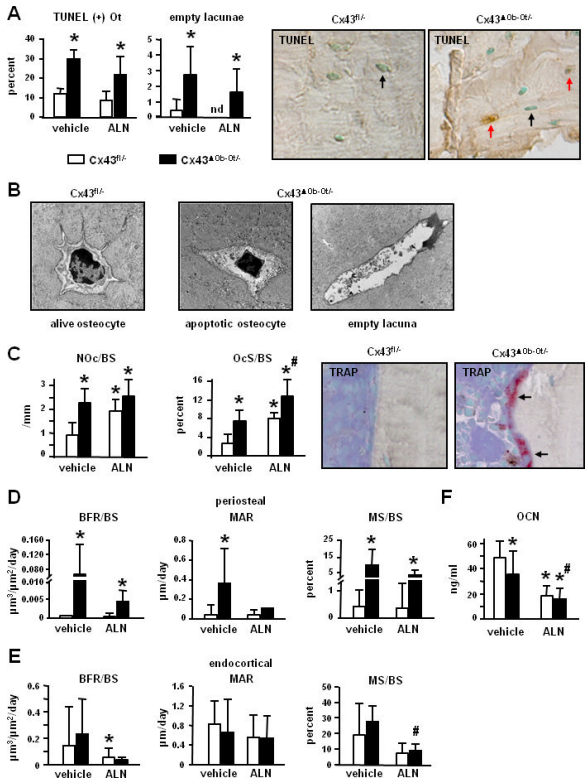


**Figure 1. Deletion of Cx43 from osteocytes and osteoblasts results in increased cortical osteocyte apoptosis, endocortical osteoclastic surface and periosteal apposition**

**(A)** Apoptotic (TUNEL positive) osteocytes were scored in the cortical bone of femora, 2.5 mm from the midshaft towards the growth plate. Representative images show examples of living (black arrows) and apoptotic (red arrows) osteocytes. ALN: alendronate. nd: non-detectable. **(B)** Representative TEM images of osteocytes in femoral midshaft**. (C)** Osteoclast number and surface were determined on the endocortical surface of the femoral midshaft. Representative images of bone sections stained for TRAP. Arrows point to TRAP positive osteoclasts. **(D** and **E)** Dynamic histomorphometric parameters were measured on the periosteal **(D)** and endocortical **(E)** surfaces of the femoral midshaft. ALN: alendronate. **(F)** Circulating levels of osteocalcin (OCN) measured in plasma. Bars are mean ± SD. * indicates significant differences versus vehicle-treated $Cx43^{fl/-}$ mice and # indicates significant differences versus vehicle-treated $Cx43^{\Delta Ob\text{-}Ot/-}$ mice at $p<0.05$, n = 6-9.

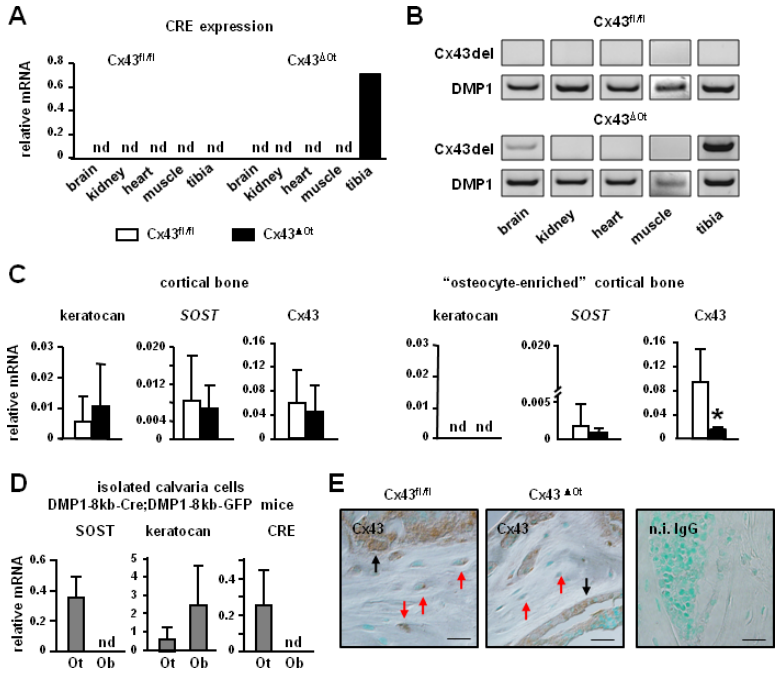


**Figure 2. Effective removal of Cx43 from osteocytes but not from osteoblasts in DMP1-8Kb-Cre;Cx43$^{fl/fl}$ (Cx43$^{\Delta Ot}$) mice**

**(A)** Cre mRNA expression in brain, kidney, heart, skeletal muscle and tibia isolated from Cx43$^{fl/fl}$ and Cx43$^{\Delta Ot}$ mice. **(B)** Genomic DNA was purified from the indicated tissues and PCR reactions for the deleted allele of Cx43 (Cx43del) and for endogenous DMP1 used as loading control. **(C)** mRNA expression of keratocan, *SOST*, and Cx43 was determined in cortical bone preparations before (left panels), and after (right panels) enzymatic digestion with collagenase in order to remove remaining osteoblasts to obtain osteocyte-enriched bone preparations. Bars are mean ± SD of five determinations (3-5 mice/preparation). * indicates significant differences versus Cx43$^{fl/fl}$ mice at $p<0.05$. **(D)** Messenger RNA expression in primary osteocytes and osteoblasts isolated from DMP1-8kb-GFP mice expressing Cre recombinase under the control of the 8kb fragment of the DMP1 promoter. OT: osteocytic cells; OB: osteoblastic cells. nd: non-detectable. Bars are mean ± SD of triplicate determinations. **(E)** Cx43 (brown) expression in femoral cortical bone of Cx43$^{fl/fl}$ and Cx43$^{\Delta Ot}$ mice stained with an anti-Cx43 polyclonal antibody or non-immune (n.i.) IgG, and counterstained with 0.2% methyl green to reveal cell nuclei (green). Red arrows point to osteocytes and black arrows point to osteoblasts. Representative sections from 3 different animals per genotype are shown. Bar indicates 20 μm.

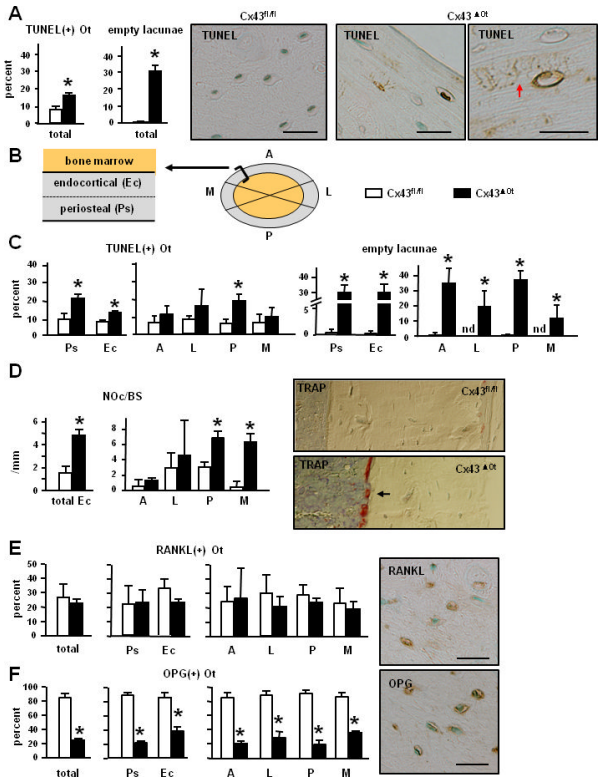


**Figure 3. Removal of Cx43 in Cx43$^{\Delta Ot}$ mice causes increased osteocyte apoptosis localized to the posterior portion of the femoral cortex, accompanied by targeted osteoclast recruitment**

(**A)** Apoptotic cells were visualized by TUNEL staining (brown) in the total cortical area in sections counterstained with methyl green (green) to detect viable cells. Percentages were calculated over the sum of viable osteocytes, apoptotic osteocytes and empty lacunae. Representative images of the posterior side in specimens stained for TUNEL are shown. Higher magnification image of TUNEL positive apoptotic osteocytes showing abundant TUNEL signal within the canalicular system (red arrow), indicating the presence of fragmented DNA. Bars indicate 20 μm. **(B)** Schematic indicates the areas in which the cortical bone was divided to measure the parameters showed in this figure. Measurements were made in two equally separated halves of the cortex: periosteal region (Ps) and endocortical region (Ec). Cells were also evaluated around the longitudinal axis in four different portions: anterior (A), lateral (L), posterior (P), and medial (M). **(C)** Prevalence of osteocyte apoptosis and empty lacunae in the two halves and in the four anatomical regions of the cortex. Bars are mean ± SD. * indicates significant differences versus Cx43$^{fl/fl}$ mice at $p<0.05$, n=3-5. **(D)** Osteoclast number on the endocortex (Ec) was determined in sections stained for TRAP and counterstained with Toluidine blue. Representative images of the posterior side stained for TRAP (arrow) are shown (400X). **(E** and **F)** The prevalence of RANKL-expressing **(E)** and OPG-expressing **(F)** osteocytes was quantified in sections stained with specific antibodies. Bars are mean ± SD. * indicates significant differences at $p<0.05$ versus Cx43$^{fl/fl}$ mice, n=3-5. Representative images of femoral cross-sections stained with antibodies directed against RANKL **(E)** and OPG **(F)** in Cx43$^{fl/fl}$ mice. Bar indicates 20 μm.

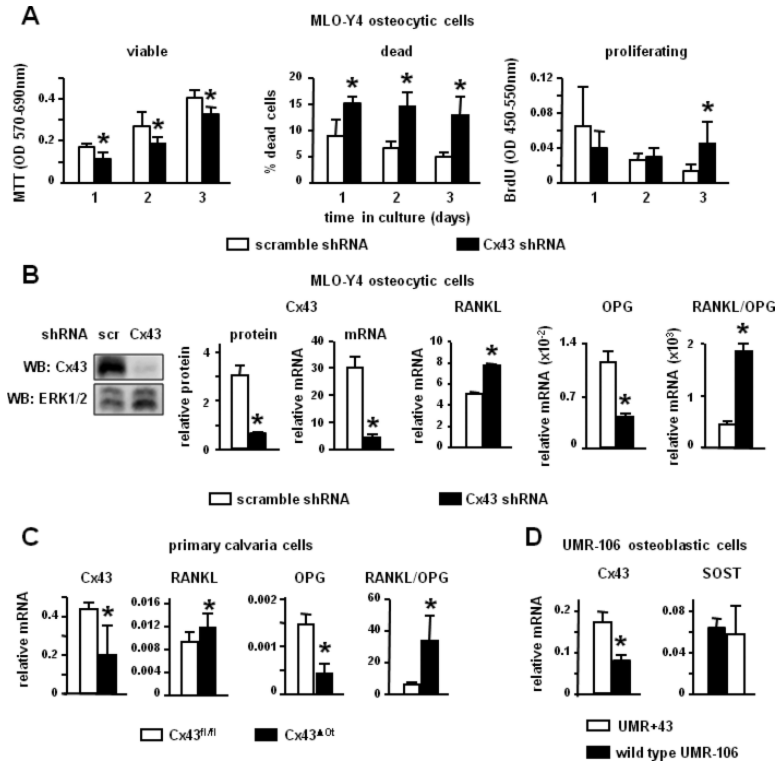


**Figure 4. Expression of Cx43 in osteocytes is required in a cell autonomous manner to maintain osteocyte viability and a low RANKL/OPG ratio *in vitro***

**(A)** Cell number, viability, and proliferation were evaluated by MTT, Trypan blue uptake, and BrdU, respectively 1, 2 and 3 days after seeding in MLO-Y4 cells silenced with scrambled or Cx43 shRNA. Each point corresponds to the mean ± SD of 6-12 replicas. * indicates significant differences versus scramble shRNA-infected cells for each time point at $p<0.05$. **(B)** Cx43 protein levels were quantified by Western blotting, corrected by ERK1/2 levels. A representative Western blot image is shown. mRNA levels for Cx43, RANKL and OPG relative to the housekeeping gene Mrps2 were determined by qPCR in MLO-Y4 expressing or not Cx43. Bars are mean ± SD of triplicate determinations. * indicates significant differences at $p<0.05$ versus scramble shRNA-infected cells. **(C)** mRNA levels for Cx43, RANKL and OPG relative to the housekeeping gene GAPDH were determined by qPCR in calvaria cells isolated from control $Cx43^{fl/fl}$ and $Cx43^{\Delta Ot}$ mice. Bars are mean ± SD of quadruplicate determinations. * indicates significant differences at $p<0.05$ versus control. **(D)** mRNA levels for Cx43 and *SOST* relative to the housekeeping gene β-actin were determined by qPCR in Cx43-transfected (UMR+43) and wild type UMR-106 cells. Bars are mean ± SD of triplicate determinations. * indicates significant differences at $p<0.05$ versus wild type cells.

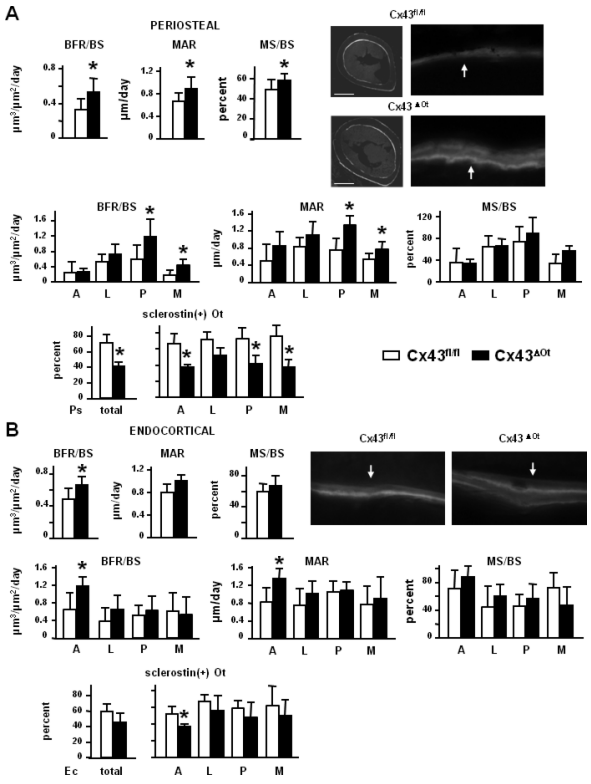


**Figure 5. Increased bone apposition in Cx43$^{\Delta Ot}$ mice coincides with surfaces adjacent to areas where sclerostin expression is low**

**(A)** Dynamic histomorphometric parameters were measured on the periosteal surface of the femoral midshaft. Bars are mean ± SD. * indicates significant differences at $p<0.05$ versus Cx43$^{fl/fl}$ mice, n=7-8. Representative images of calcein labels are shown. Left, entire cross-section at low magnification (50X), bar indicates 500 μm; right, high magnification showing the detail of the double labeling on the posterior region. Arrows point to the periosteal surface. Dynamic histomorphometric parameters in the anterior (A), lateral (L), posterior (P), and medial (M) regions around the femoral midshaft, on the periosteal surface. The prevalence of sclerostin (+) osteocytes was determined in the periosteal (Ps) half as a whole (total) and divided in the four anatomical regions, stained with anti-sclerostin antibodies and counterstained with methyl green. Bars are mean ± SD. * indicates significant differences at $p<0.05$ versus Cx43$^{fl/fl}$ mice, n=3-8. **(B)** Dymamic histomorphometric parameters were measured on the endocortical surface as a whole and divided in the four anatomical regions. Sclerostin (+) osteocytes were quantified in the endocortical half (Ec) of the bone as a whole (total) and divided in the four anatomical regions. Arrows point to the endocortical surface. Bars are mean ± SD. * indicates significant differences at $p<0.05$ versus Cx43$^{fl/fl}$ mice, n=3-8.

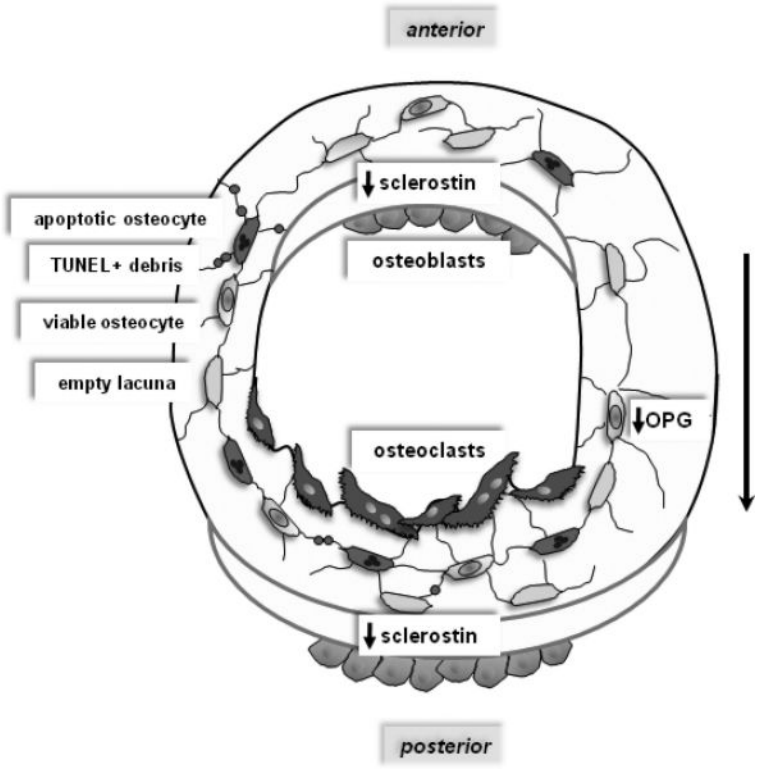


**Figure 6. Cx43 deficiency increases osteocyte apoptosis and modulates the levels of osteocytic genes that affect osteoclast and osteoblast function resulting in altered bone geometry**

Deletion of Cx43 increases apoptosis and reduces OPG gene expression in osteocytes, inducing osteoclast recruitment and resorption in the posterior endocortical area. Accumulation of empty lacunae causes a reduction in sclerostin levels with consequent increase in bone formation in the anterior endocortical surface and in the posterior periosteal surface. This results in magnification of the physiological modeling drift (represented by the arrow) by which long bones adapt their shape to mechanical needs.

## Table 1

Deletion of Cx43 from osteoblasts and osteocytes results in increased tissue, cortical, and marrow cavity area in the femoral midshaft (μCT analysis)

| | $Cx43^{fl/-}$ vehicle | $Cx43^{\Delta Ob\text{-}Ot/-}$ vehicle | $Cx43^{fl/-}$ alendronate | $Cx43^{\Delta Ob\text{-}Ot/-}$ alendronate |
|---|---|---|---|---|
| **Total tissue area ($mm^2$)** | 2.63 ± 0.32 | 3.32 ± 0.15* | 2.56 ± 0.25 | 3.23 ± 0.17* |
| **Marrow cavity area ($mm^2$)** | 1.53 ± 0.31 | 2.10 ± 0.16* | 1.26 ± 0.18* | 1.63 ± 0.12# |
| **Cortical area ($mm^2$)** | 1.10 ± 0.09 | 1.22 ± 0.13* | 1.30 ± 0.11* | 1.60 ± 0.23*# |
| **Cortical thickness (mm)** | 0.22 ± 0.02 | 0.21 ± 0.02 | 0.25 ± 0.02* | 0.28 ± 0.03*# |
| **$I_{min}$ ($mm^4$)** | 0.31 ± 0.12 | 0.43 ± 0.10* | 0.27 ± 0.06 | 0.41 ± 0.07* |
| **Bone density (pixels)** | 227.87 ± 6.86 | 223.45 ± 5.63 | 227.30 ± 5.28 | 219.71 ± 4.60* |

Values are mean ± SD.

* indicates significant differences versus vehicle-treated $Cx43^{fl/-}$ mice

# indicates significant differences versus vehicle-treated $Cx43^{\Delta Ob\text{-}Ot/-}$ mice at $p<0.05$, n = 6-10

## Table 2

Deletion of Cx43 from osteoblasts and osteocytes does not affect cancellous bone micro-architecture in the distal femur (μCT analysis)

| | $Cx43^{fl/-}$ | $Cx43^{\Delta Ob\text{-}Ot/-}$ |
|---|---|---|
| **BV/TV (%)** | 14.25 ± 5.28 | 15.72 ± 8.18 |
| **Trabecular separation (mm)** | 0.06 ± 0.01 | 0.07 ± 0.01 |
| **Trabecular number (N/mm)** | 2.22 ± 0.78 | 2.22 ± 1.18 |
| **Trabecular thickness (mm)** | 0.22 ± 0.02 | 0.21 ± 0.02 |

Values are mean ± SD, n = 6-10.

## Table 3

Deletion of Cx43 from osteocytes is sufficient to induced increased tissue, cortical, and marrow cavity area of femoral midshaft (μCT analysis)

| | $Cx43^{fl/fl}$ | $Cx43^{\Delta Ot}$ |
|---|---|---|
| **Total area ($mm^2$)** | 2.06 ± 0.25 | 2.48 ± 0.12* |
| **Marrow cavity area ($mm^2$)** | 1.28 ± 0.19 | 1.62 ± 0.10* |
| **Cortical area ($mm^2$)** | 0.77 ± 0.08 | 0.86 ± 0.05* |
| **Cortical thickness (mm)** | 0.15 ± 0.00 | 0.15 ± 0.00 |
| **$I_{min}$ ($mm^4$)** | 0.20 ± 0.05 | 0.30 ± 0.04* |
| **Bone density (pixels)** | 213.05 ± 8.42 | 213.34 ± 5.75 |

Values are mean ± SD.

* indicates significant differences versus $Cx43^{fl/fl}$ mice at $p<0.05$, n = 9-7.

## Table 4

Deletion of Cx43 from osteocytes does not affect cancellous bone micro-architecture in the distal femur (μCT analysis)

| | $Cx43^{fl/fl}$ | $Cx43^{\Delta Ot}$ |
|---|---|---|
| **BV/TV (%)** | 9.91 ± 4.01 | 9.66 ± 3.57 |
| **Trabecular thickness (mm)** | 0.05 ± 0.01 | 0.05 ± 0.00 |
| **Trabecular number (N/mm)** | 1.94 ± 0.65 | 2.05 ± 0.64 |
| **Trabecular separation (mm)** | 0.22 ± 0.02 | 0.22 ± 0.03 |

Values are mean ± SD, n = 8-7.